SIGNIFICANCE OF DEFORMATION BAND-LIKE STRIKE-SLIP FAULTS ON MARS. K. S. Artita[1] and R. A. Schultz, Geomechanic-Rock Fracture Group, Department of Geological Sciences & Engineering/172, Mackay School of Earth Sciences & Engineering, University of Nevada, Reno, NV, 89557-0138. [1]kimby@mines.unr.edu.

Introduction: Strike-slip faulting on Mars is not uncommon. Previously, it has been identified based on photographic evidence of strike-slip fault-related topographic [1], stratigraphic [2], and wrinkle ridge offsets [3], and recently, from MOLA-based DEM's [4,5]. We present new MOLA-, MDIM-, and THEMIS-based observations of strike-slip faults in East Coprates Planum (-19°S to -31°S, 300° to 310°). Unlike compressive echelon stepovers that produce push-up ridges [1], strike-slip faults in the south of the region have backward-breaking shear structures [6] at their stepovers. In order to investigate how these geometries formed, we evaluated the orientations of near-surface stress-states based on the orientations of adjacent wrinkle ridges and compared the topography of both normal and backward-breaking strike-slip stepovers. We also introduce the concept of dilatancy angle to explain the varying orientations of strike-slip faults to the maximum compressive principal stress and demonstrate, using topographic profiles across the study area, that faults in the south occur in a depositional basin. Our results indicate that strike-slip faults in the southern region behave like deformation bands, structures commonly found in porous, granular materials.

East Coprates Planum strike-slip faults: Previous mapping efforts in the area focused on wrinkle ridges that trend N-S [7-10] and strike-slip faults that trend NE-SW or NW-SE [1,8,11]. We re-mapped the region using MOLA DEM's (~279 m/pixel), MDIM's (231 m/pixel), and THEMIS' IR (100 m/pixel) (**Fig.1**).

Northern strike-slip faults. North of -25.5°S (**Fig. 1**), our mapping efforts agree well with previously published work. In this area: 1) wrinkle ridges trend approximately N-S (average 86°); 2) Sense of slip can be determined by the relationship of strike-slip fault segments to adjacent wrinkle ridges. For a left-lateral fault, thrust faults and related folds are expected to form in the second and fourth quadrants where horizontal compressive stresses accumulate; 3) Strike-slip arrays are defined by echelon segments that have polygonal or rhombohedral shaped hills or plateaus (push-up ridges) at their stepovers (**Fig. 2A-B**, **4A-B**). This local high topography is due to mechanical interaction between fault segments. Ridges produced by strike-slip arrays are thus morphologically distinct from wrinkle ridges; 4) Stepovers have forward breaking geometries meaning that stepovers in a right-stepping configuration will pinch-out to the right and vice versa (**Fig. 4A-B**); 5) Cross-cutting relationships between the wrinkle ridges and strike-slip arrays suggest the timing of deformation was broadly coeval. Most wrinkle ridges appear to have nucleated as the result of strike-slip deformation while some appear to be cross-cut by faults; 6) The overall orientation of strike-slip arrays differ from the orientation of individual segments. Fault segments are also orientated obliquely (~60°) to the overall trend of the wrinkle ridges.

Southern strike-slip faults. South of -25.5°S: 1) wrinkle ridges trend NE-SW (average 80°); 2) Strike-slip arrays have echelon segments with backward-breaking geometries at their stepovers (**Fig. 2C-D**, **4C-D**) and push-up ridges are not always observed; 3) The highest topography occurs along the bounding and linking segments instead of at the centers like push-up ridges (**Fig. 4C-D**). Arrays in this area are thus morphologically distinct from both wrinkle ridges and strike-slip arrays in the in the north; 4) Cross-cutting relationships between wrinkle ridges and strike-slip arrays suggest broadly coeval deformation; 5) The overall orientation of the strike-slip arrays differ from the overall orientation of individual segments and are highly oblique (~70°) to the trend of adjacent wrinkle ridges.

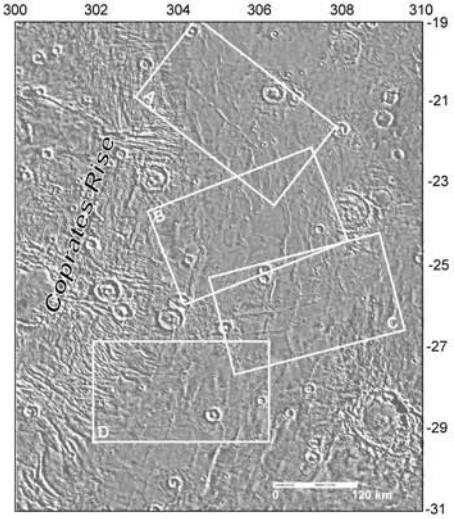

Fig. 1 - MDIM of East Coprates Planum. Location of sub-areas A-D (see **Fig. 2**)

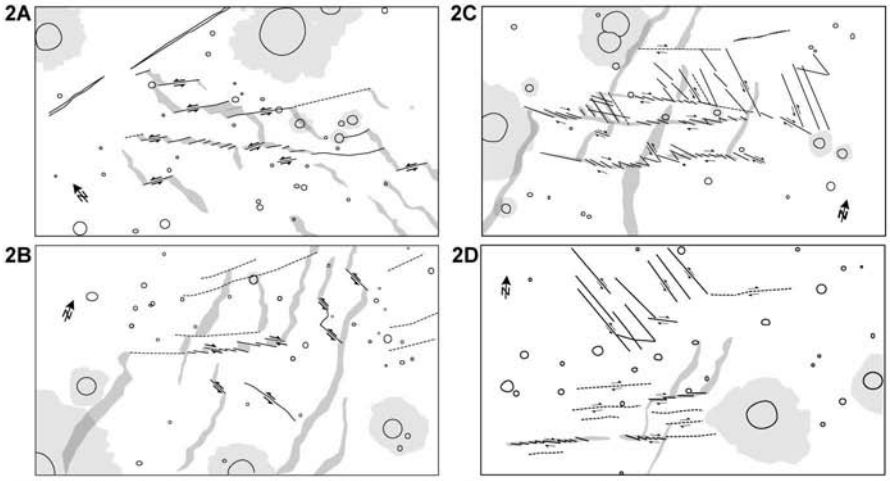

Fig. 2 - Map of sub-areas A-D. **Fig. 2A-2B** - Strike-slip arrays have "normal" breaking geometries and push-up ridges at their stepovers. **Fig. 2C-2D** - Strike-slip arrays have "backward" breaking geometries similar to those found at the compressive stepovers of deformations bands on Earth.

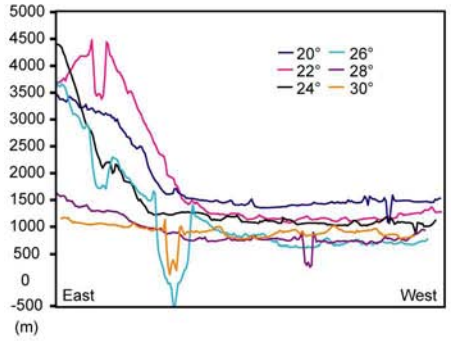

Fig. 3 - E-W profiles across E Coprates Planum from MOLA DEM's. Normal strike-slip faults (**Fig. 4A**) are found at higher latitudes (north of 25.5°). Deformation band-like strike-slip faults (**Fig. 4B**) are found at lower latitudes where there is a decrese in elevation.

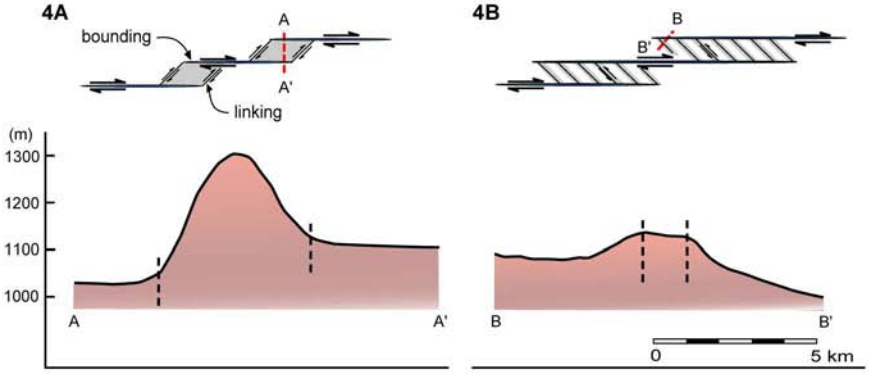

Fig. 4A - Geometry and profile of northern forward-breaking strike-slip faults. Black dashed line in profile shows approximate location of bounding fault segments. **Fig. 4B** - Geometry and topographic profile of southern backward-breaking strike-slip faults. Black dashed lines show locations of bounding and linking segments. Similar geometries have been observed on Earth in granular materials.

Fault orientation. The Mohr-Coulomb prediction of the optimal failure angle of a strike-slip fault, given by $\theta_C = 45° + \varphi/2$, is 60°, where the friction angle $\varphi = 30°$ and θ_C is the angle between the normal to the structure and the direction of the most compressive principal stress σ_1 (recall that θ_C is 60° in the north and 70° in the south). Based on our forward-modeling of wrinkle ridge topography, σ_1 is perpendicular to the strike of near-surface thrust faults. Wrinkle ridges throughout the region are parallel to the Coprates Rise (**Fig. 1**) and indicate that: 1) σ_1 rotates clockwise from the north to the south; and 2) the region was deformed under the same remote stress state. Although, the Mohr-Coulomb prediction adequately explains the orientations of strike-slip faults in the northern region [1], it does not explain orientations found in the south because if $\theta_C = 70°$, then φ is an unrealistically high value of 50°.

In summary, there is an N-S division in strike-slip array morphology in the study area. In the north, classic, forward breaking arrays are oriented at an optimal angle for Mohr-Coulomb frictional slip. In the south, strike-slip arrays are oriented at smaller angles to σ_1 which can not be explained by Mohr-Coulomb criteria. Strike-slip arrays in the south also have backward- breaking geometries at segment stepovers and bear a striking resemblance to deformation band-type arrays [12-14] studied on Earth [15-17] and when viewed in the mode-II (shear) direction [6].

Deformation bands: In granular materials, the optimal failure angle of a shear band can be expressed as [18]: $\theta = 45° + \psi/2$, where ψ is the dilatancy angle. In the southern region, for $\theta = 70°$, ψ is a realistic value of 50° [19]. Deformation bands (shear bands, Lüder's bands) form in porous granular materials on Earth such as soils, sandstones, and pyroclastic tuffs. Deformation bands are a type of fracture that initially lacks a distinctive surface of displacement discontinuity and are instead thin, planar to curviplanar zones that accommodate displacement sub-parallel to their surfaces [15]. Formation of a deformation band generally precedes fault formation in porous rocks.

Are southern faults in a depositional basin? Topographic profiles across the study area indicate that south of -25.5°S, fault segments are exposed at lower elevations than those at latitudes north of -25.5°S (**Fig. 3**). The southern region is therefore likely to be a depositional basin where granular, volcaniclastic sediments may have collected.

Implications: The geometry of a strike-slip array depends on whether the deformation is predominantly strain-softening (i.e. faults) or strain-hardening (i.e. deformation bands). Our identification of both modes in East Coprates Planum indicates a strain-softening rock type (such as basalt) in the northern region and a strain-hardening rock type (such as poorly to well indurated volcaniclastic sediments) in the south. The region southeast of the Coprates Rise might therefore be a significant sedimentary basin containing deposits comparable to the interior layered deposits of Valles Marineris. Identification of deformation bands elsewhere on Mars can reveal physical conditions such as remote stress state and lithology at the time of deformation.

References: [1] Schultz (1989) *Nature, 341,* 424-426. [2] Forsythe and Zimbelman (1998) *Nature, 336,* 14-146. [3] Anguita et al. (2001) *JGR, 106,* 20563-20585. [4] Tanaka et al. (2003) *JGR, 108*, doi:10.1029/2002JE001908. [5] Okubo and Schultz (2004) *LPS XXXV,* Abstract #1101. [6] Schultz and Balasko (2003) *GRL, 30*, doi:10.1029/2002GL018449. [7] Watters (1988) *JGR, 93,* 10235-10254. [8] Mangold et al. (1998) *Planet Space Sci, 46,* 345-356. [9] Schultz (2002) *JGR*, *105*, 12035-12052. [10] Okubo and Schultz (2004) *GSA Bulletin, 116*, 594-605. [11] Schultz and Tanaka (1994) *JGR, 99,* 8371-8385. [12] Aydin (1978) *Pure Appl Geophys, 116,* 913-930. [13] Aydin and Johnson (1983) *JSG, 5,* 19-31. [14] Antonellini et al. (1995) *JSG, 16,* 941-959. [15] Davis (1999) *Geol Soc Am Spec Pap 342.* [16] Davis et al. (2000) *JSG, 22,* 169-190. [17] Ahlgren (2001) *JSG, 23,* 1203-1214. [18] Roscoe (1970) *Géotechnique, 20,* 129-170. [19] Besuelle and Rudnicki (2004) in *Mechanics Fluid-Saturated Rocks*, 219-321.

Abstract published in: Lunar and Planetary Science XXXVI, CD-ROM, Lunar and Planetary Institute, Houston (2005).